Ionic Transport and Thermodynamic Interaction in Precision Polymer Blend Electrolytes for Lithium Batteries

Kyoungmin Kim[1,2,=], Nam Nguyen[3,=], Stephanie F. Marxsen[1], Sage Smith[1,2], Rufina G. Alamo[1], Justin G. Kennemur[3,*], Daniel T. Hallinan Jr.[1,2,*]

[1] Department of Chemical and Biomedical Engineering, Florida A&M University–Florida State University (FAMU-FSU) College of Engineering, 2525 Pottsdamer Street, Tallahassee, Florida 32310, USA
[2] Aero-propulsion, Mechatronics and Energy (AME) Center, FAMU-FSU College of Engineering, 2003 Levy Avenue, Tallahassee, Florida 32310, USA
[3] Department of Chemistry and Biochemistry, Florida State University, 95 Chieftan Way, Florida 32306, USA

[=]Contributed equally to this work.
[*]Corresponding authors.
[*]jkennemur@fsu.edu, dhallinan@eng.famu.fsu.edu

Keywords: Single-ion conductor, polyelectrolyte, precise, polyanion, solid electrolyte, charged polymer blend, Flory-Huggins interaction parameter, melting point depression, Chi

Abstract

Single-ion conducting polymer electrolytes are of interest for use with advanced battery electrodes such as lithium metal, but achieving sufficiently high conductivity has been challenging. In this work, a model system containing charged sites that are precisely spaced along the polymer backbone is explored. Precision sulfonated poly(4-phenylcyclopentene) lithium salt (*p*5PhS-Li) with a high degree of sulfonation (> 90%) was synthesized and blended with poly(ethylene oxide) (PEO) to investigate the thermodynamic and transport properties. Melting point depression was measured via differential scanning calorimetry, ionic conductivity κ,was determined using electrochemical impedance spectroscopy, and the fraction of current carried by Li^+ was estimated based on steady-state current measurements. In conjunction with a density measurement, melting point depression was used to find an effective Flory-Huggins interaction parameter, $\chi_{eff} = -0.21$, suggesting miscibility of the blend. κ spanned a large range from 2×10^{-11} to 2×10^{-7} S cm^{-1} over the composition and temperature range investigated. The fraction of charge carried by lithium ions also spanned a significant range from 0.12 in majority PEO blend to 0.98 in majority *p*5PhS-Li blend. This

study addresses several limitations of sulfonated polystyrene and opens up the possibility of precisely controlling the spacing of other anion types.

Introduction

Conventional liquid electrolytes have been in use since the 1990s in commercial lithium-ion batteries.[1] However, the reactivity and instability with advanced electrodes like lithium metal are major concerns that require further research for alternative replacements.[1, 2] Polymer electrolytes have been gaining interest for the past few decades due to safety enhancement, good flame retardation, excellence in thermal and electrochemical stability, low-cost production, and potential compatibility with high specific energy electrodes in lithium batteries.[3-7] The basic design of a polymer electrolyte consists of lithium salt mixed into a polymer matrix, most commonly poly(ethylene oxide) (PEO).[8, 9] However, salt concentration gradients form in such dual-ion conductors, which have detrimental effects on the performance of lithium-ion batteries such as voltage losses and high internal impedance (reducing energy efficiency) as well as side reactions that can cause cell failure.[10-12] One way to mitigate this is to create single-ion conductors (SICs), in which the counter anions are immobilized by covalent bonding to a polymer (i.e. polyelectrolytes), that allow lithium ions to be the only mobile ion. However, one of the main challenges of dry SICs is poor ionic conductivity. Some component is needed to facilitate ion dissociation, which is achieved using dry rubbery polar polymers, such as PEO. Lithium ions dissociate from the polyelectrolyte due to coordination with PEO. The mobility of the ions is dictated by the segmental motion of the polymer chains.[9, 13, 14] One of the most studied precursors for SICs is polystyrene (PS) due to its ease in synthesis and the versatile chemical modifications to the phenyl rings.[15, 16] However, the high glass transition temperature (T_g) of PS-based SICs hinders the segmental mobility of miscible blends (and block copolymers) with PEO. In other words, conductivity suffers due to the correlation between ion mobility and chain dynamics and the reduction in chain mobility when blended with rigid, PS-based, SICs. As a result, sulfonated PS-based polymer blend electrolytes have conductivities of 10^{-6} to 10^{-7} S cm^{-1} at 90 °C; conductivity can be increased 2 orders of magnitude by incorporating large, charge delocalized anionic moieties.[16, 17] Even so, these values are below desired ionic conductivity for commercial purposes that liquid electrolytes can provide ($>10^{3}$ S cm^{-1} at room temperature).[18, 19]

Recently, poly(4-phenylcyclopentene) (P4PCP) was synthesized and the backbone olefins were saturated through hydrogenation (H2-P4PCP).[20] The novelty of this material is that every phenyl group is spaced exactly five carbons on a linear hydrocarbon (polyethylene-like) backbone.[20] For simplicity, this manuscript will describe H2-P4PCP as *p*5Ph, which represents a precise polyethylene with a phenyl branch at every 5 backbone carbons. The increased spacing between phenyl groups drastically decreases the T_g of *p*5Ph to 17 ˚C.[20] Soon after, *p*5Ph was successfully sulfonated (95% of repeating units) and neutralized with a variety of counter cations to produce a unique set of precision polyelectrolytes that feature the 5-carbon charge spacing.[21] We envisioned that the increase in segmental mobility of these SICs, supplied by the lower T_g of *p*5Ph, would lead to an increase in ionic conductivity when compared to their PS counterparts.

The miscibility of PEO and polyelectrolytes has not been thoroughly studied. Since PEO is essential for lithium ions to dissociate from the SICs, its miscibility with polyelectrolytes can directly affect the dissociation state of lithium ions and their conductivity.[4] In order to combine the polymers for our study, blending was utilized as it is a classic, low-cost technique that can combine the properties of both homopolymers to create a novel polymeric material. In this article, we prepared blends of sulfonated *p*5Ph neutralized with a lithium counter-cation (*p*5PhS-Li) and PEO with varying weight fractions to study the miscibility, ionic conductivity, and fraction of charged carried by Li^+ using a variety of characterization methods.

Experimental

Materials

Dimethyl sulfoxide (DMSO, ≥ 99.9% anhydrous), hexane (≥ 98.5%, ACS reagent), chloroform (≥ 99.9%, HPLC Plus), benzaldehyde (≥ 99.0%, ReagentPlus), titanium (IV) tetrachloride (≥ 99.9%, trace metal basis), Hoveyda-Grubbs 2nd generation catalyst (HG2, 97.0%), Grubbs 1st generation catalyst (G1, 97%) ethyl vinyl ether (EVE, 99.0%), *o*-xylene (≥ 98%, ACS reagent), tributylamine (≥ 98.5%, ACS reagent), benzene (≥ 99.0%, ACS reagent), and sulfuric acid (95.0-98.0%, ACS reagent) were purchased from Sigma-Aldrich and used as received. Allyltrimethylsilane (96.0%), *p*-toluenesulfonyl hydrazide (95.0 %) were purchased

from Oakwood Chemicals and used as received. Nitromethane (99.0%, Oakwood Chemicals) was dried by distillation over $CaCl_2$. Anhydrous lithium hydroxide (99.995%, trace metal basis) was used as received from Beantown chemical. DMSO-d_6 was purchased from Alfa Aesar and used as received. Dry toluene and dichloromethane were obtained from an SG Waters glass contour solvent purification system by passage through columns packed with neutral alumina followed by a 2 μm filter. *p*5PhS-Li was dried at 140 °C under vacuum for 48 h. PEO (M_n = 20 kg mol^{-1}, Sigma-Aldrich) was dried at 60 °C under vacuum for 24 h. After drying, *p*5PhS-Li and PEO were transferred into an argon-filled glovebox without exposure to air. Preparation of polymer blends and electrolytes was conducted in the argon-filled glovebox with O_2 and H_2O levels less than 0.2 ppm.

Synthesis of p5PhS-Li

Details of the synthesis of *p*5PhS-Li have been previously reported.[21] For the specific material reported herein, the parent polymer, *p*5Ph, was determined to have a number averaged molar mass (M_n) of 17 kg mol^{-1} and a dispersity ($Đ$) of 1.67 via size exclusion chromatography (SEC). Full synthesis and characterization details are provided in the Supporting Information. The degree of sulfonation was determined to be 90 ± 3 % by triplicate titrations with a 9.48 mM solution of NaOH previously calibrated with potassium phthalate. *p*5PhS-Li was generated by adding an aqueous solution containing 0.95 g of polymer into dialysis tubing and submerging within 4 L of a 0.1 M aqueous solution of LiOH for 48 h followed by subsequent dialysis in deionized water to remove excess LiOH. The number average degree of polymerization (N_n) for the parent *p*5Ph is 116 and, based on the degree of sulfonation, the final M_n of *p*5PhS-Li was calculated to be 24 kg mol^{-1}, using the molar mass of the *p*5PhS-Li repeat unit (232.25 g mol^{-1}). In prior work, we have shown that the sulfonation and neutralization procedure is not deleterious to the molar mass and dispersity of the parent polymer.[21]

Preparation of polymer blends

Blend compositions ranging from 90% to 10% (w/w PEO) with *p*5PhS-Li were prepared in glovebox and are visually illustrated in Scheme 1. For each blend, approximately 100 mg was

made by dissolving calculated amounts of *p*5PhS-Li and PEO in 500 µL of anhydrous DMSO. The solutions were cast on a nickel foil-covered hot plate set to 60 °C and dried for 48 h. The films produced were further dried *in vacuo* for another 24 h at 60 °C before characterization. All blend compositions were coded as EO_x *p*5PhS-Li_y in which subscripts *x* and *y* represent the weight fraction of each component, respectively. The blend compositions and cation concentrations are shown in Table 1.

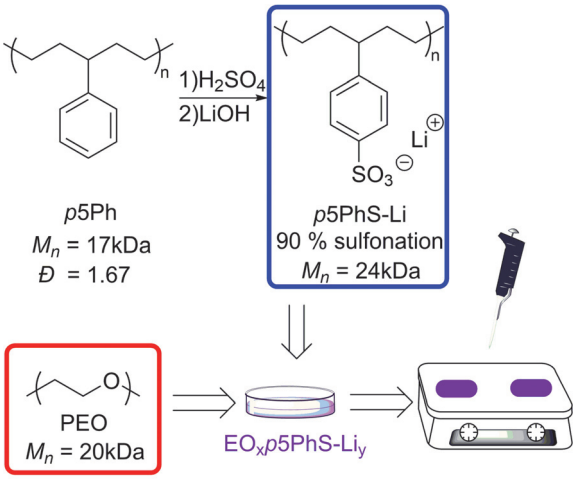

Scheme 1. Simplified, visual sample preparation of EO_x*p*5PhS-Li_y blends

Table 1. Blend composition and concentration

Blend	$r = [Li^+]/[EO]$	$[Li^+]:[EO]$
$EO_{0.9}$ *p*5PhS-$Li_{0.1}$	0.02	1:50
$EO_{0.7}$ *p*5PhS-$Li_{0.3}$	0.08	1:12
$EO_{0.5}$ *p*5PhS-$Li_{0.5}$	0.19	1:5
$EO_{0.3}$ *p*5PhS-$Li_{0.7}$	0.44	1:2
$EO_{0.1}$ *p*5PhS-$Li_{0.9}$	1.71	1:0.5

Density measurement of p5PhS-Li

The density of *p*5PhS-Li was measured by sink – float tests with mixtures of chloroform (1.48 g cm^{-3}) and hexane (0.67 g cm^{-3}) in order to find the molar volume of *p*5PhS-Li repeat units.

Various mole fractions of chloroform and hexane solutions were prepared in 4 mL scintillation vials, and the density of the solutions were calculated from previously reported literature with the temperature of the solution being 24 ± 1 °C.[22] Bulk pieces of *p*5PhS-Li were submerged in the non-solvent solutions and gently shaken to liberate any surface bubbles. Then the polymer was released to observe sinking or floating behavior in the solution. The density of *p*5PhS-Li was determined to be 1.33 ± 0.01 g cm^{-3} at 24 ± 1 °C. The standard deviation of the density measurement was determined by averaging 5 density measurements to ensure reproducibility. We determined a 0.001 g cm^{-3} error from temperature uncertainty, which we deem negligible.

Differential scanning calorimetry (DSC)

A known mass (~5 mg) of each blend composition was dissolved in 40 µL of anhydrous DMSO and cast directly in an aluminum DSC pan. The pans were heated at 60 °C inside the glovebox for 48 h before being dried *in vacuo* at 60 °C for another 24 h before being hermetically sealed. Thermal and crystallization behavior was measured with a TA Q2000 equipped with RC900 intracooler and operated under dry nitrogen gas. Samples were cycled between -80 °C and 90 °C at a rate of 10 °C min^{-1} and data was taken on the second heating and replicated 3 times.

Electrochemical measurements

Polymer electrolyte films were prepared using Garolite spacers with thickness of 127 µm (0.005 in). The spacers were prepared using hollow punches to have an outer diameter of 12.7 mm (1/2 in) and an inner diameter of 3.175 mm (1/8 in). The polymer blends were loaded in the spacers and pressed at 60 °C. The average thickness of the polymer electrolyte films was 200 ± 20 µm. Lithium-lithium symmetric cells were assembled by placing lithium metal electrodes (diameter: 4.76 mm = 3/16 in) on each side of a polymer blend/spacer assembly. Nickel current collectors were attached to both lithium electrodes. The cells were sealed in laminated aluminum pouch material using a vacuum sealer. At least 3 cells were assembled for each blend composition.

The cells were annealed in a convection oven (Heratherm, Thermo Scientific) at 90 °C for 12

h followed by conditioning cycles. Small currents of ± 2 μA cm^{-2} were alternately applied to the cells for 4 h with intervening 2 h rests to introduce stable interfacial layers in the conditioning process. The ionic conductivities of the polymer electrolytes were measured by galvanostatic electrochemical impedance spectroscopy (EIS) with 10 nA of alternating current and frequency from 1 MHz to 100 mHz. EIS was conducted at temperatures from 40 °C to 90 °C in the convection oven. At each temperature, 3 measurements were performed with 3 h isothermal equilibration and 1 h rest between the measurements. Potentiostatic polarization was also conducted at temperatures from 70 to 90 °C, by applying constant voltage of 200 mV to the cells for 1 h.

Results

Differential scanning calorimetry

The second heating scans from DSC measurements are shown in Figure S9. An endothermic peak was observed for all of the compositions, and this is attributed to the melting of PEO.

The degree of crystallinity normalized per mass of PEO (X_c), can be calculated according to Equation (1):

$$X_c = \frac{\Delta H_m}{w_{PEO}\Delta H_m^0} \times 100\% \quad (1)$$

in which w_{PEO} represents weight fraction of PEO in the blends, ΔH_m^0 represents the melting enthalpy of pure PEO with 100% crystallinity, and ΔH_m represents enthalpy of melting measured by DSC. Due to a wide variety of reported values of ΔH_m^0 that range between 196 J g^{-1} and 210 J g^{-1}, an average value of 203 J $g^{-1}$was used.[23-26]

Table 2. DSC data of PEO and p5PhS-Li blends with varying compositions.

Sample	Mass (mg)	T_m (°C)	ΔH_m (J g_{sample}^{-1})	X_c (%)
Pure *p*5PhS-Li	-	-	-	-
$EO_{0.1}$ *p*5PhS-$Li_{0.9}$	4.2	58.9 ± 1.8	7.6 ± 2.2	39 ± 9%
$EO_{0.3}$ *p*5PhS-$Li_{0.7}$	4.3	59.6 ± 0.5	31.4 ± 5.2	52 ± 7%
$EO_{0.5}$ *p*5PhS-$Li_{0.5}$	3.6	61.0 ± 0.9	75.6 ± 2.1	75 ± 2%
$EO_{0.7}$ *p*5PhS-$Li_{0.3}$	4.7	61.9 ± 0.8	100.2 ± 3.4	70 ± 2%
$EO_{0.9}$ *p*5PhS-$Li_{0.1}$	3.9	62.9 ± 0.4	160.0 ± 3.3	87 ± 2%

Pure PEO	4.8	64.4 ± 1.1	178.1 ± 0.3	88 ± 1%

Results of the DSC study are summarized in Table 2. The melting temperature (T_m) was taken as the peak maximum. Integration of the area under the melting peak, along with the mass of the sample, was used to determine ΔH_m and calculate the degree of crystallinity according to Equation (1). As *p*5PhS-Li is amorphous, the heat of fusion is normalized by the weight fraction of crystalline PEO in the blend. X_c decreased with increasing *p*5PhS-Li content in the blend with the most pronounced effect occurring at high *p*5PhS-Li compositions. The T_m of PEO is depressed by the addition of *p*5PhS-Li as illustrated in Figure S10 where T_m is plotted against the weight fraction of *p*5PhS-Li in the blend, $w_{p5\mathrm{PhS-Li}}$. The T_m of PEO decreases from 64 °C to 59 °C from pure PEO ($w_{p5\mathrm{PhS-Li}} = 0$) to 10 wt% PEO ($w_{p5\mathrm{PhS-Li}} = 0.9$).

On the assumption of compatibility of the polymer blends studied, the melting point depression is associated with the Flory-Huggins interaction parameter, χ. [27, 28] Assuming reasonably high degrees of polymerization (greater than 100) such as those used in this study (454 for PEO, 116 for *p*5PhS-Li), the melting point composition expression for polymer-diluent mixtures equation can be written as[29, 30]

$$\left(\frac{1}{T_{m,PEO}} - \frac{1}{T_{m,blend}}\right) = \frac{RV_2}{V_1 \Delta H_m^0} \chi (\phi_1)^2 \qquad (2)$$

where $T_{m,PEO}$ is the melting point of pure PEO, $T_{m,blend}$ is the melting point of PEO in different blend compositions, R is the universal gas constant, V_2 is the molar volume per repeat unit of semicrystalline component (PEO), V_1 is the molar volume per repeat unit of the diluent (*p*5PhS-Li), and ϕ_1 is the volume fraction of *p*5PhS-Li. The following values were used to calculate the interaction parameter: V_2 = 39.3 cm^3 mol^{-1} that is obtained by using the density of amorphous PEO at room temperature,[31, 32] ΔH_m^0 = 8942 J mol^{-1},[33, 34] and V_1 = 174.6 cm^3 mol^{-1} based on the density of *p*5PhS-Li and molar mass of a repeat unit. The data from Figure S10 are plotted according to Equation (2) in Figure 1. By plotting $\left(\frac{1}{T_{m,PEO}} - \frac{1}{T_{m,blend}}\right)$ against $(\phi_1)^2$ the slope can be obtained that represents $\frac{RV_2}{V_1 \Delta H°(PEO)} \chi$. Since Flory-Huggins (and Lattice)

theory[28] does not account for specific interactions such as those between ions and dipoles, we refer to the obtained interaction parameter as χ_{eff}.[35] The χ value obtained is -0.21 ± 0.04. The detailed calculation is included in the Supporting Information.

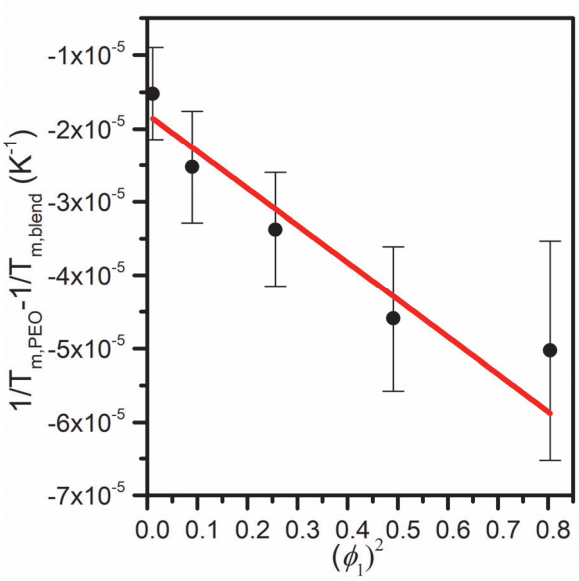

Figure 1. Plot according to Equation (2) as a function of the square of the *p*5PhS-Li volume fraction. Solid line is a linear fit. Error bars represent standard deviations of ($1/T_{m,PEO} - 1/T_{m,blend}$) that was obtained from different measurements of $T_{m,PEO}$ and $T_{m,blend}$

Ionic conductivity

The ionic conductivity (κ) was calculated by

$$\kappa = \frac{L}{AR_b}, \tag{3}$$

where L is the electrolyte thickness (cm), A is the area (cm^2) of the electrolyte, and R_b is the bulk resistance in Ohms ($\Omega = S^{-1}$) obtained from the Nyquist plot, which represents the imaginary (-Im(Z)) versus real part (Re(Z)) of the complex resistance (impedance). Representative Nyquist plots at 60 and 65 °C of EIS measurements of $EO_{0.5}$ *p*5PhS-$Li_{0.5}$ are shown in Figure 2. Below T_m, low-frequency impedance was not measured due to the high resistance of the samples exceeding the limit of the instrument. The Nyquist plot above T_m (65 °C) showed two semicircles. The high-frequency semicircle corresponds to bulk electrolyte resistance. The low-frequency semicircle corresponds to a combination of charge transfer resistance and interfacial resistance.[36] R_b was therefore determined by fitting the high frequency data to an equivalent circuit with a resistor, R1, and a capacitor, C1, in a parallel

circuit shown in the inset of Figure 2(a).

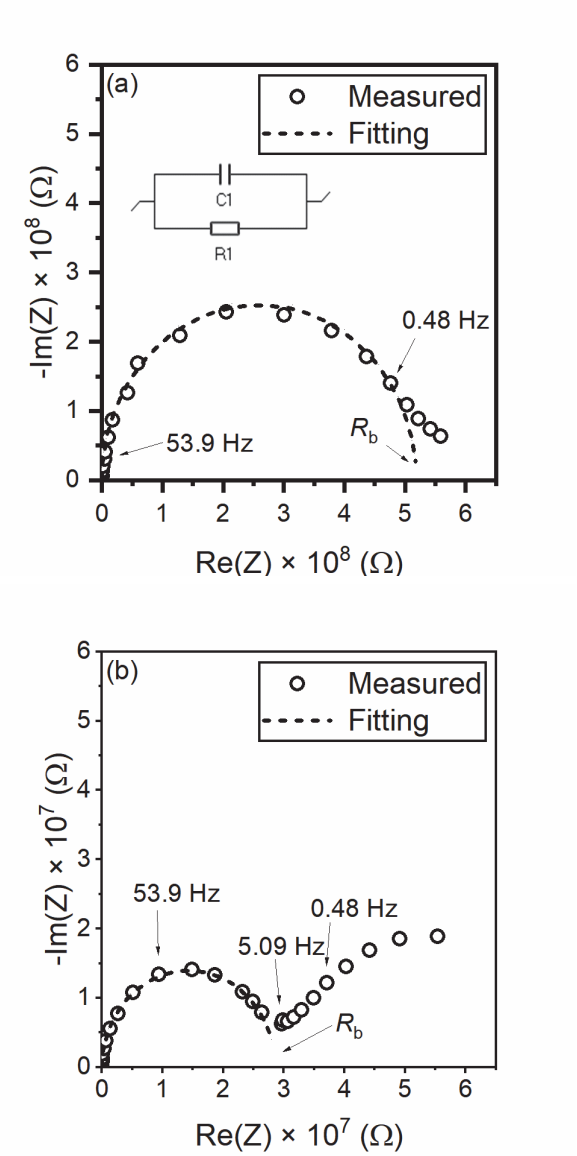

Figure 2. Nyquist plot of $EO_{0.5}$*p*5PhS-$Li_{0.5}$ at (a) 60 and (b) 65 °C with indication of frequency and R_b. The equivalent circuit used for fitting (dashed semicircles) is presented in the inset of (a).

The representative ionic conductivities of the three blend compositions with $w_{p5\mathrm{PhS-Li}}$ of 0.1, 0.5, and 0.9 are shown in Figure 3. The ionic conductivities of all blends are reported in Table S10. The ionic conductivities were between 10^{-11} to 10^{-10} S cm^{-1} at 40 °C and 10^{-8} to 2 × 10^{-7} S cm^{-1} at 90 °C. The ionic conductivity showed a sharp increase and large standard deviation

from 55 to 70 °C where the PEO crystallites melt. The increase in conductivity when heating from 55 to 70 °C was less prominent at low EO composition ($EO_{0.1}$ *p*5PhS-$Li_{0.9}$). The ionic conductivity of $EO_{0.1}$ *p*5PhS-$Li_{0.9}$ was the lowest between 70 and 90 °C but higher than the others (except $EO_{0.9}$ *p*5PhS-$Li_{0.1}$) between 40 and 55 °C.

The ionic conductivities below T_m (40 – 55 °C) were fitted by the Arrhenius model,

$$\kappa = \kappa_0 \exp\left(-\frac{E_a}{RT}\right) \quad (4)$$

where κ_0 is the pre-exponential factor and E_a is the activation energy. The Arrhenius parameters are shown in Table 3, and the fitting results are presented as solid lines in Figure 3 (a). $EO_{0.1}$ *p*5PhS-$Li_{0.9}$ showed highest activation energy.

The data above T_m (70 – 90 °C) was fit to the Vogel-Fulcher-Tammann (VFT) model,

$$\kappa = \kappa_0 \exp\left(\frac{-B}{T-T_0}\right) \quad (5)$$

where B is E_a/R and T_0 is a fitting parameter associated with the temperature at which all mobility ceases. The VFT parameters are shown in Table 3, and the fitting results are presented as solid curves in Figure 3 (a). The blend with the highest *p*5PhS-Li concentration ($EO_{0.1}$ *p*5PhS-$Li_{0.9}$) exhibited Arrhenius behavior ($T_0 = 0$). The ionic conductivity of $EO_{0.1}$ *p*5PhS-$Li_{0.9}$ across the entire temperature range was fitted to the Arrhenius model and the result is shown in Figure 3 (a) (black dashed line). The κ_0 and E_a of $EO_{0.1}$ *p*5PhS-$Li_{0.9}$ were 3.65×10^6 S cm^{-1} and 100.22 kJ/mol, respectively.

The concentration dependence of ionic conductivity is shown in Figure 3 (b). $EO_{0.9}$ *p*5PhS-$Li_{0.1}$ showed 10 times higher ionic conductivity than the other blends between 70 and 90 °C. For all temperatures, local maxima were found at $w_{p5\mathrm{PhS-Li}} = 0.5$. The non-monotonic behavior of the concentration dependence is discussed in the next section.

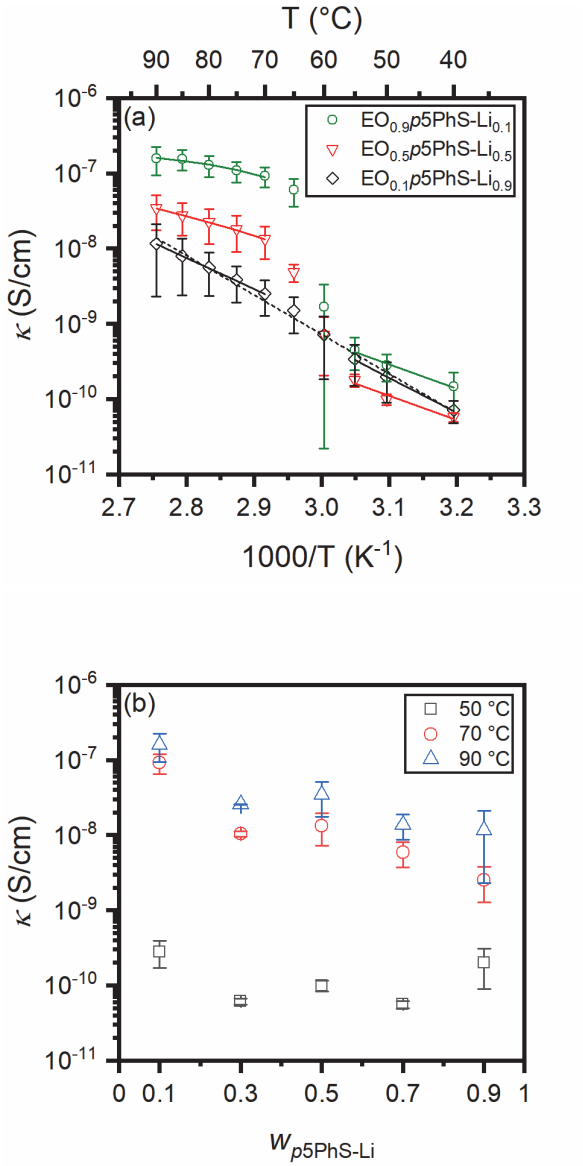

Figure 3. (a) Ionic conductivity (κ) of representative *p*5PhS-Li/PEO blends as a function of temperature. Solid lines are Arrhenius fits for 40 to 55 °C. Solid curves are VFT fits for 70 to 90 °C. Dashed line is Arrhenius fit from 40 to 90 °C. (b) Ionic conductivity (κ) of *p*5PhS-Li/PEO blends as a function of composition.

Table 3. Arrhenius and VFT Fitting Parameters

Model	Parameter	$EO_{0.9}$ *p*5PhS-$Li_{0.1}$	$EO_{0.7}$ *p*5PhS-$Li_{0.3}$	$EO_{0.5}$ *p*5PhS-$Li_{0.5}$	$EO_{0.3}$ *p*5PhS-$Li_{0.7}$	$EO_{0.1}$ *p*5PhS-$Li_{0.9}$
Arrhenius (40 – 55 °C)	κ_0 **(S cm^{-1})**	3.49	4847	1.01	88	39435
	E_a **(kJ mol^{-1})**	62.28	86.29	61.53	75.47	88.40
	R^2	0.9819	0.9989	0.9302	0.9807	0.9986
VFT (70 - 90 °C)	κ_0 **(S cm^{-1})**	3.54×10^{-7}	5.39×10^{-6}	3.10×10^{-6}	1.68×10^{-7}	2.23×10^{3}
	E_a **(kJ mol^{-1})**	0.31	7.42	4.40	1.65	78.49
	T_0 **(K)**	316.2	209.0	246.0	284.1	0
	R^2	0.9683	0.9998	0.9984	0.9996	0.9995

Figure 4 shows the results of potentiostatic polarization of *p*5PhS-Li/PEO blends with lithium electrodes. Figure 4 (a) is a representative current profile of $EO_{0.5}$ *p*5PhS-$Li_{0.5}$ at 90 °C and 0.2 V for 1 h. The initial and steady-state current were denoted as I_0 and I_{ss}, respectively. The ratio of I_{ss} and I_0 (I_{ss}/I_0) are shown in Figure 4 (b). $EO_{0.1}$ *p*5PhS-$Li_{0.9}$ showed the highest value of I_{ss}/I_0 (0.98) implying single-ion conduction while $EO_{0.9}$ *p*5PhS-$Li_{0.1}$ showed the lowest value (0.12) implying higher anion mobility than cation mobility.

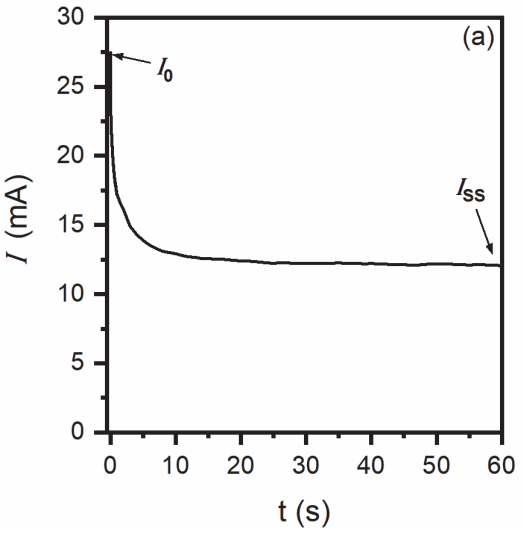

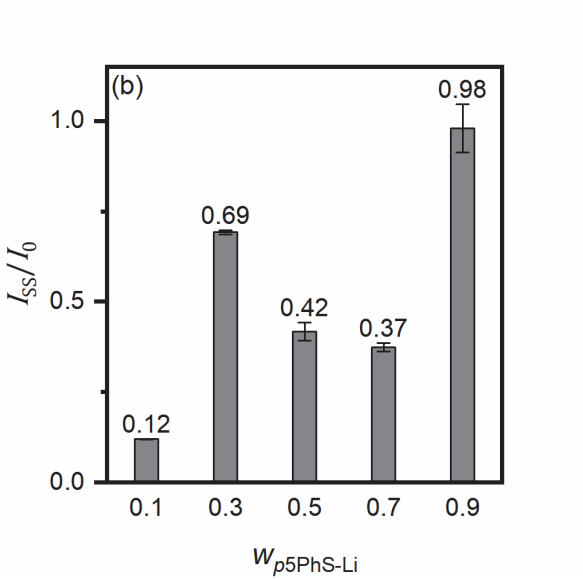

Figure 4. (a) Potentiostatic polarization of $EO_{0.5}$ *p*5PhS-$Li_{0.5}$ at 90 °C, (b) I_{ss}/I_0 of *p*5PhS-Li/PEO blends at 90 °C.

Discussion

For blends that are generally accepted as highly immiscible, such as poly(propylene)/poly(polystyrene) or poly(propylene)/poly(2,6-dimethyl-1,4-phenylene oxide), X_c of the semicrystalline component remains unperturbed with the increase in amorphous component.[37, 38] However, our system shows a reduction of PEO X_c with increasing *p*5PhS-Li compositions. The introduction of *p*5PhS-Li into PEO at higher compositions had a greater effect on reducing X_c values as shown in Table 2. For example, the $EO_{0.1}$ *p*5PhS-$Li_{0.9}$ and $EO_{0.3}$ *p*5PhS-$Li_{0.7}$ blends showed a X_c that was 48 and 35% lower than pure PEO, respectively. This trend did not continue below 70 wt% of *p*5PhS-Li, where the reduction in X_c is less than 20%.

A possible explanation for this behavior is that these blends exhibit complex miscibility at the molar masses, compositions, and temperatures used in this study. This is bolstered by a negative, yet weak, χ parameter (-0.21). In the bulk state, *p*5PhS-Li has been recently shown to nanophase separate into percolated ionic networks driven by the flexible yet non-polar nature of the PE backbone/phenyl rings versus the precisely-spaced polar regions of the neutralized sulfonate species.[39] These networks are persistent over a large temperature range. Combining

this nanophase self-assembly with another component (PEO) may be resulting in complex phase behavior of these blends at the varying compositions studied. For example, at low PEO compositions, $EO_{0.1}$ *p*5PhS-$Li_{0.9}$ and $EO_{0.3}$ *p*5PhS-$Li_{0.7}$, blending into *p*5PhS-Li may lead to a co-existence of the percolated networks swelled by the low quantity of PEO. At higher PEO loadings, these networks may be ruptured and the system behave as a miscible or partially miscible blend. It is worth pointing out that the local maximum that occurs not only in κ but also in X_c occurs at an ion content where incomplete miscibility has been observed between PEO and lithium salts.[40] Thus, both components of the blend electrolyte may play a role in the apparent complexity of its physical properties. More studies will be needed to fully understand the phase behavior of these two polymers.

For PEO and polyolefins like PE, both A and B are large and positive in $\chi_{eff} = A + \frac{B}{T}$ so that χ_{eff} is positive at all temperatures. For PEO and PS, $\chi_{eff} = -1.73 \times 10^{-2} + \frac{23.7}{T[K]}$.[41] The positive value of B indicates that no attractive interactions exist between PEO and PS. In fact, χ_{eff} is positive at all temperatures below the degradation temperature. Therefore, the only source of associative interactions between PEO and *p*5PhS-Li can be attributed to ion-dipole interactions between the lithium sulfonate species and ether groups. Intermolecular interactions such as dipole-dipole and ion-dipole can promote miscibility and disrupt PEO crystallinity by promoting dissolution of lithium ions (and polyelectrolyte) into PEO. This is reflected in the negative χ_{eff} that, although a crude measure of molecular interactions,[42] is the empirical value used to quantify the experimental data in hand. The weakly negative value of χ_{eff} may be due not only to the hydrophobicity of the *p*5PhS-Li backbone but also the strong intermolecular interactions of SO_3^- undermining both lithium ion dissociation and crystallinity suppression. Similar behavior has been observed in blends of PEO and lithium poly(styrene sulfonate) (PSSLi), in which PEO retains high crystallinity and the T_g of neat PEO has been detected in the blends.[43, 44] Unlike sulfonate anions, larger and more delocalized anions such as trifluoromethylsulfonyl imide (TFSI) have been shown to suppress PEO crystallinity.[16, 34] It also exhibits increased ionic conductivity at room temperature due to charge delocalization.[16, 45, 46] The smaller and less charge-delocalized anions of *p*5PhS-Li and *p*SSLi

are not expected to fully disrupt crystallinity of PEO, which is verified by DSC results.

Another indication of blend miscibility is the T_m depression of the semicrystalline component.[29] Based on Equation (2), the magnitude of the interaction parameter as well as the melting point depression depend on the strength of polymer-polymer interaction. The melting point of PEO decreases from 64 °C for pure PEO to 59 °C at $EO_{0.1}$ *p*5PhS-$Li_{0.9}$, from which a χ value of -0.21 was obtained. The negative value for χ indicates thermodynamically favorable mixing between the two components.[47, 48] Here we acknowledge that V_1 was obtained at 24 °C and there may be some discrepancy associated with the actual molar volume at T_m. Recent literature reports an interaction parameter of -1.15 between methacrylic sulfonyl imide derived polyelectrolyte (PLiMTFSI) and PEO with the melting point depression going from 69 °C to 62 °C at only 30 wt% polyelectrolyte.[34] In contrast, our blend compositions exhibit a narrower melting point depression range (5 °C) with larger compositions of study. The magnitude of T_m depression for PLiMTFSI/PEO is larger than that observed in our study, which indicates PLiMTFSI/PEO has greater compatibility. The exact determination of phase behavior in polymer blends cannot be deduced only by DSC experiments as it has been shown to be complicated by blend compositions and ionic interactions.[49, 50] Nonetheless, the experimental results indicate some degree of miscibility, which must be the case for the blends to exhibit higher ionic conductivity than that of neat *p*5PhS-Li due to the dissociation of lithium ions into PEO. Neat *p*5PhS-Li exhibits at least 2 orders lower ionic conductivity[39] at the same measured temperature as *p*5PhS-Li/PEO blends at all compositions.

According to our observations, the temperature dependence of the ionic conductivity can be separated into 3 regions based on the T_m of PEO: below T_m (≤ 55 °C), through T_m (55-70 °C), and above T_m (≥ 70 °C). Above T_m, the ionic conductivity is between 10^{-9} and 10^{-7} S cm^{-1}, which is 3 to 5 orders of magnitude lower than PEO-based polymer electrolytes.[40] The goodness of the VFT fits for intermediate blend compositions above T_m indicate that ion transport occurs by segmental motion of ethylene oxide, in agreement with observations of other PEO-based polymer electrolytes.[9] PEO segmental motion which is slowed by ion coordination such that the ionic conductivity depends in a complex way on the mole ratio of lithium to EO ($[Li^+]/[EO]$, *r*). Previous studies on PEO/lithium salt electrolytes have reported

maximum ionic conductivities at r = 0.085.[40] For PSSLi/PEO blends, the maximum ionic conductivities were found at r = 0.125.[44, 51] This is understood as that the *p*SSLi/PEO blends have lower number of free cations for the same r value due to the strong interaction between the Li^+ and SO_3^- group resulting in poor dissociation of cations from the polymer backbone. In this study, the maximum ionic conductivity was found at the lowest limit (r = 0.02, $EO_{0.9}$ *p*5PhS-$Li_{0.1}$) and a local maximum was found at r = 0.19 ($EO_{0.5}$ *p*5PhS-$Li_{0.5}$) which is even higher than that of *p*SSLi/PEO systems. The significantly higher ionic conductivity of the blend at r = 0.02 than other compositions is attributed to diffusion of entire *p*5PhS-Li chains. At this composition, the blend is liquid-like above PEO T_m, indicative of chain diffusion. Based on a scaling approximation the reptation time is a function of the number of entanglements cubed and the Rouse relaxation time of an entanglement strand: $\tau_{rep} \approx \left(\frac{M_n}{M_e}\right)^3 \tau_e$. For PEO $M_e \approx 2{,}000$ g mol^{-1}, and $\tau_e = 1.5 \times 10^{-8}$ s at 75 ℃.[52] Thus, $\tau_{rep} \approx 1.5 \times 10^{-5}$ s for 20,000 g mol^{-1} PEO at 75 ℃. Presumably, the parent precision polymer, *p*5Ph, and therefore p5PhS-Li have an entanglement molecular weight between that of PS (17,000 g mol^{-1}) and polyethylene (1,000 g mol^{-1}),[53] such that the number of entanglements per chain is probably less than that of PEO. There is much more uncertainty regarding τ_e of *p*5PhS-Li. In any case, the reptation time for blends that are dilute in *p*5PhS-Li would be expected to be dominated by PEO dynamics, i.e. entanglements are rapidly released by PEO chain diffusion so that p5PhS-Li chains can also diffuse.

At higher *p*5PhS-Li concentration, ion transport is thought to be lower due to the increased viscosity of the blends, with the blend becoming solid-like at a composition of $EO_{0.3}$ *p*5PhS-$Li_{0.7}$. Despite $EO_{0.3}$ *p*5PhS-$Li_{0.7}$ containing more ions, $EO_{0.5}$ *p*5PhS-$Li_{0.5}$ exhibited higher ionic conductivity due presumably to having greater ion mobility.

Above T_m and $w_{p5PhS-Li} \geq 0.5$, the ionic conductivity decreased with increasing lithium concentration. This is thought to be due to a saturation of EO coordination sites such that there are diminishing returns of free ions with increasing *p*5PhS-Li content as well as a dominance of the high T_g *p*5PhS-Li on ion dynamics.[40] Note that although the neutral parent polymer

has a T_g below room temperature, the T_g of *p*5PhS-Li is above the degradation temperature, i.e. undetectable. Strong dependence of apparent T_g on ionic form of polyelectrolytes has been widely observed.[54] The values of ionic conductivity of *p*5PhS-Li/PEO blend was an order of magnitude lower compared to PSSLi/PEO blends while the flexible *p*5PhS-Li backbone was expected to improve the ion mobility. For the same *r* value, the weight fraction of PEO of *p*5PhS-Li/PEO blend is lower than that of PSSLi/PEO due to the higher molecular weight of repeating unit of *p*5PhS-Li. Since *p*5PhS-Li and PSSLi have high T_g, the difference in repeat unit molar mass is thought to cause reduced segmental motion of *p*5PhS-Li/PEO blends as well as reduced volume fraction of conducting phase as compared to PSSLi/PEO at the same *r* value. The more hydrophobic backbone of *p*5PhS-Li may also play a role.[21]

The ionic conductivities below T_m were 1 to 2 orders of magnitude lower than those above T_m because segmental and chain motion is limited due to PEO crystallization so that ion hopping dominates the cation transport. Based on the activation energy from the Arrhenius and VFT parameters, no significant difference was found in temperature dependence between the blends with *p*5PhS-Li weight fraction of 0.1 to 0.7 (Table 3). However, $EO_{0.1}$*p*5PhS$Li_{0.9}$ showed a distinguishable temperature dependence: Arrhenius behavior across the entire temperature range (40-90 °C). It is thought that the amorphous phase of PEO matrix cannot have more influence on the ion transport when $w_{p5PhS\text{-}Li}$ is 0.9 because the PEO phase is perhaps enclosed by *p*5PhS-Li and ion hopping through the *p*5PhS-Li dominates the transport.

The hypothesis that the dominant transport mechanism relies on blend composition can be supported by potentiostatic polarization results. In Figure 4, the low value of I_{ss}/I_0 of $EO_{0.9}$ *p*5PhS-$Li_{0.1}$ indicates that the anion is highly diffusive. Since the sulfonate groups on the polymer chain are the only anions in this study, we concluded that the *p*5PhS-Li polymer chains diffuse through the PEO matrix. For $EO_{0.1}$ *p*5PhS-$Li_{0.9}$, the I_{ss}/I_0 was highest and close to unity. This is due to the fact that transport of anions is limited by fixed rigid *p*5PhS-Li matrix. The I_{ss}/I_0 values of *p*5PhS-Li/PEO blends between 0.3 to 0.7 of $w_{p5PhS-Li}$ were 0.3 – 0.7, which are between two extremes of $EO_{0.9}$ *p*5PhS-$Li_{0.1}$ and $EO_{0.1}$ *p*5PhS-$Li_{0.9}$. The values showed decreasing trend with increasing $w_{p5PhS-Li}$. It is worth noting that the correction using

impedance to take into account the passivation layer during potentiostatic polarization for the conventional Bruce-Vincent[55] method was not conducted because the interfacial impedance was undetectably high. Therefore, the factors that makes decreasing I_{ss}/I_0 between 0.3 to 0.7 of $w_{p5\mathrm{PhS-Li}}$ are not elucidated in this paper. It could be coupled with the build-up of internal resistance due to local polarization in the immiscible, but partially compatible blend, different lithium stripping/plating kinetics due to the different compositions and physical properties, and polymer segmental dynamics.

Conclusions

Newly synthesized precision *p*5PhS-Li and *p*5PhS-Li/PEO blends were investigated in terms of their thermodynamic and electrochemical properties. A weak melting point depression and PEO crystallinity reduction with increasing content of *p*5PhS-Li in the blends, indicated an at least partial miscibility of both components. The ionic conductivity, κ, was measured by EIS, and the temperature dependence was found to depend on the amount of amorphous phase. Values of I_{ss}/I_0 indicated high mobility of polyanions at the highest PEO content and single-ion conduction at highest *p*5PhS-Li content. The ion transport is thought to be dominated by chain diffusion at the highest PEO content, by ion hopping at the highest *p*5PhS-Li content, or by segmental motion at intermediate compositions. It is expected that the study of structure-properties relationships will clarify the role of precise charge spacing in development of single-ion conducting polymer electrolytes.

Acknowledgments

The authors would like to acknowledge Matthew Lundblad for the DSC discussion. This work was supported by the National Science Foundation, award number 1804871.

References

[1] G. E. Blomgren, *Journal of the Electrochemical Society* **2017**, *164*, A5019.
[2] J. M. Tarascon, M. Armand, *Nature* **2001**, *414*, 359.
[3] M. Armand, J. M. Tarascon, *Nature* **2008**, *451*, 652.

[4] A. A. Rojas, S. Inceoglu, N. G. Mackay, J. L. Thelen, D. Devaux, G. M. Stone, N. P. Balsara, *Macromolecules* **2015**, *48*, 6589.
[5] J. L. Thelen, S. Inceoglu, N. R. Venkatesan, N. G. Mackay, N. P. Balsara, *Macromolecules* **2016**, *49*, 9139.
[6] D. H. C. Wong, A. Vitale, D. Devaux, A. Taylor, A. A. Pandya, D. T. Hallinan, J. L. Thelen, S. J. Mecham, S. F. Lux, A. M. Lapides, P. R. Resnick, T. J. Meyer, R. M. Kostecki, N. P. Balsara, J. M. DeSimone, *Chemistry of Materials* **2015**, *27*, 597.
[7] D. T. Hallinan, S. A. Mullin, G. M. Stone, N. P. Balsara, *Journal of the Electrochemical Society* **2013**, *160*, A464.
[8] Z. Xue, D. He, X. Xie, *Journal of Materials Chemistry A* **2015**, *3*, 19218.
[9] D. T. Hallinan Jr, N. P. Balsara, *Annual review of materials research* **2013**, *43*, 503.
[10] J. N. Chazalviel, *Physical Review A* **1990**, *42*, 7355.
[11] R. P. Doyle, X. Chen, M. Macrae, A. Srungavarapu, L. J. Smith, M. Gopinadhan, C. O. Osuji, S. Granados-Focil, *Macromolecules* **2014**, *47*, 3401.
[12] J. Newman, K. E. Thomas-Alyea, "*Electrochemical Systems"*, 3rd edition, Wiley-Interscience, Hoboken, NJ 2004, p. 647.
[13] D. E. Fenton, J. M. Parker, P. V. Wright, *Polymer* **1973**, *14*, 589.
[14] O. Borodin, G. D. Smith, *Macromolecules* **2006**, *39*, 1620.
[15] C. H. Park, Y.-K. Sun, D.-W. Kim, *Electrochimica Acta* **2004**, *50*, 375.
[16] Q. Ma, Y. Xia, W. Feng, J. Nie, Y.-S. Hu, H. Li, X. Huang, L. Chen, M. Armand, Z. Zhou, *RSC advances* **2016**, *6*, 32454.
[17] R. Meziane, J.-P. Bonnet, M. Courty, K. Djellab, M. Armand, *Electrochimica Acta* **2011**, *57*, 14.
[18] N. Kamaya, K. Homma, Y. Yamakawa, M. Hirayama, R. Kanno, M. Yonemura, T. Kamiyama, Y. Kato, S. Hama, K. Kawamoto, A. Mitsui, *Nature Materials* **2011**, *10*, 682.
[19] W.-S. Young, W.-F. Kuan, I. I. I. T. H. Epps, *Journal of Polymer Science Part B: Polymer Physics* **2014**, *52*, 1.
[20] W. J. Neary, J. G. Kennemur, *Macromol. Rapid Commun.* **2016**, *37*, 975.
[21] A. Kendrick IV, W. J. Neary, J. D. Delgado, M. Bohlmann, J. G. Kennemur, *Macromolecular rapid communications* **2018**, *39*, 1800145.
[22] I. C. Wei, R. L. Rowley, *Journal of Chemical & Engineering Data* **1984**, *29*, 332.
[23] A. R. Polu, H.-W. Rhee, D. K. Kim, *Journal of Materials Science: Materials in Electronics* **2015**, *26*, 8548.
[24] G. Zardalidis, J. Mars, J. Allgaier, M. Mezger, D. Richter, G. Floudas, *Soft Matter* **2016**, *12*, 8124.
[25] E. Salmon, S. Guinot, M. Godet, J. F. Fauvarque, *Journal of Applied Polymer Science* **1997**, *65*, 601.
[26] M. Minelli, M. G. Baschetti, D. T. Hallinan, Jr., N. P. Balsara, *Journal of Membrane Science* **2013**, *432*, 83.
[27] P. J. Flory, *Journal of Chemical Physics* **1949**, *17*, 223.
[28] P. J. Flory, "*Principles of polymer chemistry"*, Cornell University Press, 1953.
[29] T. Nishi, T. T. Wang, *Macromolecules* **1975**, *8*, 909.
[30] P. B. Rim, J. P. Runt, *Macromolecules* **1984**, *17*, 1520.
[31] D. Walsh, P. Zoller, "*Standard pressure volume temperature data for polymers"*, CRC press, 1995.
[32] J. L. Thelen, X. C. Chen, S. Inceoglu, N. P. Balsara, *Macromolecules* **2017**, *50*, 4827.
[33] A. T. Lorenzo, M. L. Arnal, J. Albuerne, A. J. Müller, *Polymer Testing* **2007**, *26*, 222.
[34] J. L. Olmedo-Martínez, L. Porcarelli, Á. Alegría, D. Mecerreyes, A. J. Müller, *Macromolecules* **2020**, *53*, 4442.
[35] P. C. Hiemenz, T. P. Lodge, "*Polymer Chemistry Second Edition"*, CRC Press, Boca Raton, 2007.

[36] M. D. Berliner, B. C. McGill, M. Majeed, D. T. Hallinan Jr., *Journal of The Electrochemical Society* **2019**, *166*, A1.
[37] S. Jose, A. S. Aprem, B. Francis, M. C. Chandy, P. Werner, V. Alstaedt, S. Thomas, *European Polymer Journal* **2004**, *40*, 2105.
[38] S. Paszkiewicz, A. Szymczyk, P. Franciszczak, I. Taraghi, D. Pawlikowska, R. Jeziórska, *Polymer Bulletin* **2018**, *75*, 3679.
[39] B. A. Paren, B. A. Thurston, W. J. Neary, A. Kendrick, J. G. Kennemur, M. J. Stevens, A. L. Frischknecht, K. I. Winey, *Macromolecules* **2020**, *53*, 8960.
[40] S. Lascaud, M. Perrier, A. Vallee, S. Besner, J. Prudhomme, M. Armand, *Macromolecules* **1994**, *27*, 7469.
[41] H. B. Eitouni, N. P. Balsara, "Thermodynamics of Polymer Blends", in *Physical Properties of Polymers Handbook*, Second edition, J.E. Mark, Ed., Springer, New York, 2007.
[42] C. E. Sing, M. O. de la Cruz, *ACS Macro Letters* **2014**, *3*, 698.
[43] M. Martinez-Ibañez, E. Sanchez-Diez, L. Qiao, L. Meabe, A. Santiago, H. Zhu, L. A. O'Dell, J. Carrasco, M. Forsyth, M. Armand, H. Zhang, *Batteries & Supercaps* **2020**, *3*, 738.
[44] C. H. Park, Y. K. Sun, D. W. Kim, *Electrochimica Acta* **2004**, *50*, 375.
[45] S. Feng, D. Shi, F. Liu, L. Zheng, J. Nie, W. Feng, X. Huang, M. Armand, Z. Zhou, *Electrochimica Acta* **2013**, *93*, 254.
[46] L. Porcarelli, M. A. Aboudzadeh, L. Rubatat, J. R. Nair, A. S. Shaplov, C. Gerbaldi, D. Mecerreyes, *J. Power Sources* **2017**, *364*, 191.
[47] Z. Qiu, T. Ikehara, T. Nishi, *Polymer* **2003**, *44*, 2799.
[48] H. J. Kim, X. Peng, Y. Shin, M. A. Hillmyer, C. J. Ellison, *The Journal of Physical Chemistry B* **2021**, *125*, 450.
[49] V. A. Pryamitsyn, H.-K. Kwon, J. W. Zwanikken, M. Olvera de la Cruz, *Macromolecules* **2017**, *50*, 5194.
[50] C. E. Sing, M. Olvera de la Cruz, *ACS Macro Letters* **2014**, *3*, 698.
[51] Q. Ma, Y. Xia, W. F. Feng, J. Nie, Y. S. Hu, H. Li, X. J. Huang, L. Q. Chen, M. Armand, Z. B. Zhou, *Rsc Advances* **2016**, *6*, 32454.
[52] O. Oparaji, S. Narayanan, A. Sandy, S. Ramakrishnan, D. Hallinan Jr, *Macromolecules* **2018**, *51*, 2591.
[53] M. Rubinstein, R. H. Colby, "*Polymer physics"*, Oxford university press New York, 2003.
[54] A. Kusoglu, A. Z. Weber, *Chemical Reviews* **2017**, *117*, 987.
[55] J. Evans, C. A. Vincent, P. G. Bruce, *Polymer* **1987**, *28*, 2324.

TOC Entry

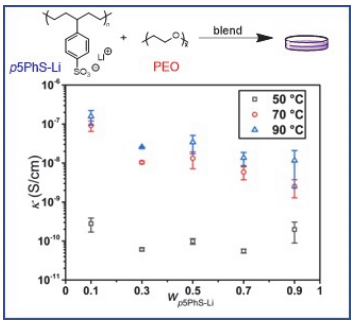

Polymer blends comprising varying amounts of precision polymer electrolyte and lithium-solvating polymer were investigated for miscibility in addition to Li-ion transference and conductivity. Insight on the mechanism of ion transport as a function of blend composition is discussed.